# Regioselective Aliphatic Carbon−Carbon Bond Cleavage by a Model System of Relevance to Iron-Containing Acireductone Dioxygenase

Caleb J. Allpress,[†] Katarzyna Grubel,[†] Ewa Szajna-Fuller,[†] Atta M. Arif,[‡] and Lisa M. Berreau*,[†]

[†]Department of Chemistry and Biochemistry, Utah State University, Logan, Utah 84322-0300, United States
[‡]Department of Chemistry, University of Utah, Salt Lake City, Utah 84112-0850, United States

S *Supporting Information*

ABSTRACT: Mononuclear Fe(II) complexes ([[(6-Ph$_2$TPA)Fe(PhC(O)-C(R)C(O)Ph)]X (**3-X**: R = OH, X = ClO$_4$ or OTf; **4**: R = H, X = ClO$_4$)) supported by the 6-Ph$_2$TPA chelate ligand (6-Ph$_2$TPA = *N,N*-bis((6-phenyl-2-pyridyl)methyl)-*N*-(2-pyridylmethyl)amine) and containing a *β*-diketonate ligand bound via a six-membered chelate ring have been synthesized. The complexes have all been characterized by ^{1}H NMR, UV−vis, and infrared spectroscopy and variably by elemental analysis, mass spectrometry, and X-ray crystallography. Treatment of dry CH$_3$CN solutions of **3-OTf** with O$_2$ leads to oxidative cleavage of the C(1)−C(2) and C(2)−C(3) bonds of the acireductone via a dioxygenase reaction, leading to formation of carbon monoxide and 2 equiv of benzoic acid as well as two other products not derived from dioxygenase reactivity: 2-oxo-2-phenylethylbenzoate and benzil. Treatment of CH$_3$CN/H$_2$O solutions of **3-X** with O$_2$ leads to the formation of an additional product, benzoylformic acid, indicative of the operation of a new reaction pathway in which only the C(1)−C(2) bond is cleaved. Mechanistic studies show that the change in regioselectivity is due to the hydration of a vicinal triketone intermediate in the presence of both an iron center and water. This is the first structural and functional model of relevance to iron-containing acireductone dioxygenase (Fe-ARD′), an enzyme in the methionine salvage pathway that catalyzes the regiospecific oxidation of 1,2-dihydroxy-3-oxo-(*S*)-methylthiopentene to form 2-oxo-4-methylthiobutyrate. Importantly, this model system is found to control the regioselectivity of aliphatic carbon−carbon bond cleavage by changes involving an intermediate in the reaction pathway, rather than by the binding mode of the substrate, as had been proposed in studies of acireductone enzymes.
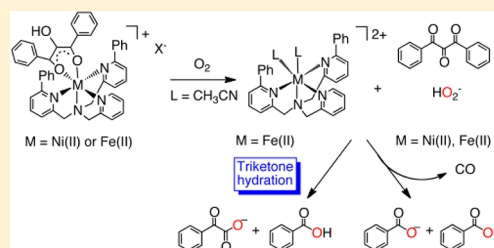
INTRODUCTION

One of the most challenging reactions in chemistry and biology is the selective oxidative cleavage of carbon−carbon bonds. The enzymes that carry out these reactions are typically dioxygenases, which incorporate two oxygen atoms into products via an oxidative mechanism and often contain a metal cofactor (typically iron) in a nonheme binding pocket.[1] While the mechanism of enzymes that cleave aromatic carbon−carbon bonds, such as the extradiol and intradiol catechol dioxygenases, have been extensively studied,[2,3] enzymes that cleave aliphatic carbon−carbon bonds have received much less attention until recently. These enzymes, which include acetylacetone-cleaving dioxygenase (Dke1),[4] 2,4′-dihydroxyacetophenone dioxygenase,[5] hydroxyethylphosphonate dioxygenase,[6] and the acireductone dioxygenases,[7] are the subject of growing interest. The acireductone dioxygenases, found in the methionine salvage pathway, are of particular current interest, due to the change in regiospecificity of the reaction as a function of metal ion bound at the active site. This differing reactivity within the enzymes as a function of metal ion identity is unique at present in biology.

The methionine salvage pathway is ubiquitous in biological systems and is responsible for regenerating methionine from 5′-methylthioadenosine.[8] In aerobic systems, this pathway contains a single branch point, wherein an acireductone intermediate (1,2-dihydroxy-3-oxo-(*S*)-methylthiopentene) undergoes a reaction catalyzed by one of two different dioxygenase enzymes (Scheme 1).[9] In the on-pathway reaction, iron-containing acireductone dioxygenase (Fe-ARD′) catalyzes the oxidative cleavage of the C(1)−C(2) bond resulting in the formation of formic acid and an *α*-keto acid, the latter of which undergoes transamination in a subsequent step to regenerate methionine. In the off-pathway reaction, nickel-containing acireductone dioxygenase (Ni-ARD) catalyzes the oxidative cleavage of the C(1)−C(2) and C(2)−C(3) bonds of the acireductone to form formic acid, carbon monoxide (CO), and a carboxylic acid.[10] The mechanism of Ni-ARD has been the focus of several recent studies, primarily through model systems, for two main reasons: (1) Nickel-containing dioxygenases were hitherto unknown; and (2) the production of CO is of particular current interest due to its role in cellular signaling.[11] In this context, the branch point in the methionine salvage pathway at which the acireductone dioxygenases operate represents a combination of a potential regulatory shunt coupled with the production of a signaling molecule.

Despite catalyzing reactions with differing regiospecificity, Fe-ARD′ and Ni-ARD contain identical peptide sequences and bind the divalent metal cofactor with the same four amino acid

Scheme 1. Regiospecificity of Aliphatic Carbon−Carbon Bond Cleavage by Acireductone Dioxygenases in the Methionine Salvage Pathway
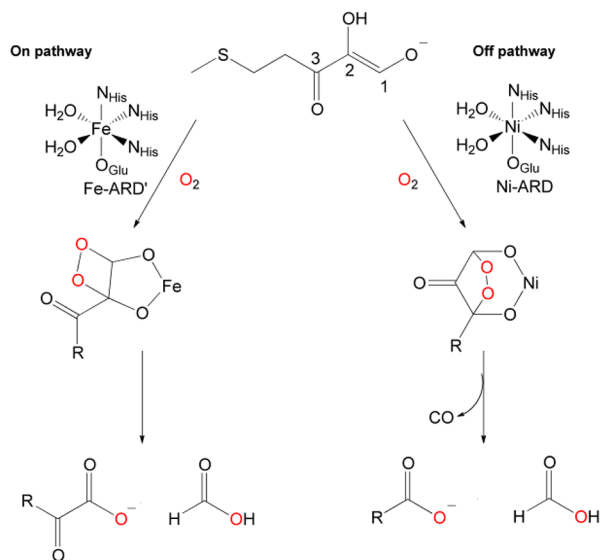
residues (3His, 1Glu).[9] Thus, the only constitutive difference for the two enzymes is the nature of the metal at the active site. To date, no model complexes have been synthesized to study the reaction pathway in Fe-ARD′.

The current hypothesis for the difference in regiospecificity is that a change in the coordination mode of the substrate from a six-membered chelate in Ni-ARD to a five-membered chelate in Fe-ARD′ results in the observed differences in reactivity of bond cleavage (Scheme 1).[9] To probe this chelate ring hypothesis, we have previously prepared a Ni(II)-containing complex of a bulky acireductone (2-hydroxy-1,3-diphenyl-propan-1,3-dione), [(6-Ph$_2$TPA)Ni(PhC(O)C(OH)C(O)-Ph)]ClO$_4$ (1), that is supported by an aryl-appended TPA ligand (6-Ph$_2$TPA = N,N-bis((6-phenyl-2-pyridyl)methyl)-N-(2-pyridylmethyl)amine) in order to mimic the hydrophobic binding pocket found in ARDs.[12] X-ray crystallographic and ^{1}H NMR solution studies of 1 revealed that the acireductone moiety in this complex is coordinated as a six-membered chelate ring. Upon treatment of 1 with O$_2$, the C(1)−C(2) and C(2)−C(3) bonds of the acireductone were cleaved, and CO was generated, in a Ni-ARD-type reaction (Scheme 2, top).

Scheme 2. (Top) Reaction of 1 with O$_2$ to Form Ni-ARD-Type Products via the Formation of an Intermediate Triketone Species and (Bottom) Decarbonylation of 1,3-Diphenylpropantrione via a Lewis Acid-Mediated Benzoyl Migration
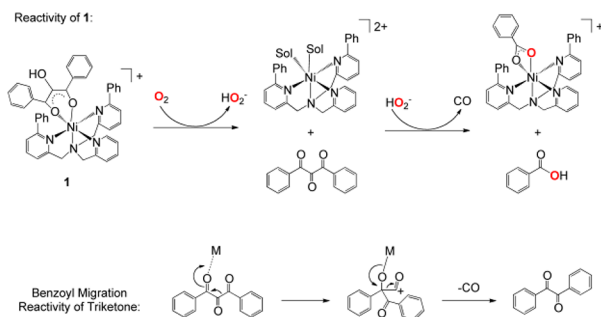
Mechanistic studies suggest this reaction proceeds by an initial net two-electron process to form 1,3-diphenylpropantrione (a vicinal triketone) and hydroperoxide anion, which may then combine to form a dioxetane ring and subsequently cleave the C−C bonds.[13] The triketone intermediate was implicated by the detection of benzil, which is formed in the reaction mixture via a benzoyl migration and decarbonylation (Scheme 2, bottom).[14] We note that the production of benzil was the only initial evidence for a reaction pathway involving a triketone intermediate. Benzoyl migration is not possible with the native ARD substrate, and so such a byproduct would not be produced in the enzyme, even if the reaction were to proceed via a triketone intermediate.

In the present work, we have investigated the role of the metal center in the O$_2$ reactivity of acireductones by utilizing an iron-containing analogue of 1. While spectroscopic studies provide evidence for a six-membered chelate ring for the coordinated acireductone, we have found that the presence of iron and water in the reaction mixture opens up a new oxidative reaction pathway not accessible in our nickel-containing system. This new reaction pathway results in the formation of benzoylformic acid, the α-keto acid product that would be expected in a Fe-ARD′ type reaction.

■ EXPERIMENTAL SECTION

General Methods. All reagents were obtained from commercial sources and were used without additional purification unless otherwise noted. The 1,3-diphenylpropantrione was purchased from TCI America. Solvents were dried according to published procedures and were purified by distillation under N$_2$ prior to use.[15] Air-sensitive reactions were performed in an MBraun Unilab glovebox under a N$_2$ atmosphere or by using standard Schlenk techniques. Fe(OTf)$_2$·2CH$_3$CN was prepared from Fe powder, and FeCl$_3$ was prepared from FeCl$_3$·6H$_2$O using known procedures.[16,17] The bulky acireductone 2-hydroxy-1,3-diphenylpropan-1,3-dione was synthesized by modifying a literature procedure as described below.[18] The 6-Ph$_2$TPA (N,N-bis((6-phenyl-2-pyridyl)methyl)-N-(2-pyridylmethyl)-amine) ligand, [(6-Ph$_2$TPA)Ni(CH$_3$CN)(H$_2$O)](ClO$_4$)$_2$, and 2-oxo-2-phenylethylbenzoate were synthesized by following previously published procedures.[19−21]

Physical Methods. ^{1}H NMR spectra of organic compounds were obtained using a JEOL ECX-300 spectrometer; chemical shifts were referenced to the residual solvent peak in CD$_2$$H$CN (1.94 ppm, quintet). ^{1}H NMR spectra of paramagnetic complexes were obtained using a Bruker ARX-400 spectrometer and parameters, as previously described.[22] UV−vis data were collected on a HP8453A spectrometer at ambient temperature. IR spectra were recorded on a Shmidzu FTIR-8400 spectrometer as KBr pellets. Room temperature magnetic susceptibilities were determined using the Evans method.[23] GC-MS data were obtained on a Shimadzu GCMS-QP5000 GC-MS with a GC-17A gas chromatograph, using an Alltech EC5 30 m × 25 mm ×25 μm thin film capillary column and temperature program: $T_{initial}$, 70 °C (5 min); temperature gradient, 23 °C min^{-1}; T_{final}, 250 °C (10 min). LC-MS data were obtained using negative-ion APCI on a LCQ Thermo Finnigan MS via a HP1100 with a Betasil C18 10 × 2.1 mm column; solvent gradient from 5% aqueous methanol to 50% aqueous methanol. CO was detected using an Agilent 3000A Micro gas chromatograph. Mass spectral data for metal complexes were collected by the Mass Spectrometry Facility, University of California, Riverside. Elemental analysis was performed by Atlantic Microlabs Inc., Norcross, GA for all compounds except 3-OTf, which was analyzed by Canadian Microanalytical Service, Ltd.

Kinetic Studies. Measurements were performed on a HP8453A spectrometer at 20 °C. All manipulations of 3-X were performed under a N$_2$ atmosphere. O$_2$-saturated solutions of CH$_3$CN (8.2 mM) were prepared by bubbling dry O$_2$ through a solution of dry CH$_3$CN.[24] Solutions containing lower O$_2$ concentrations were prepared by

diluting the 8.2 mM solution with N_2-saturated CH_3CN using gastight syringes.

Caution! Perchlorate salts of metal complexes with organic ligands are potentially very explosive. Only small amounts of material should be prepared, and these should be handled with extreme caution.[25]

2-Hydroxy-1,3-diphenyl-propan-1,3-dione. $NaHCO_3$ (1.68 g, 20.0 mmol) was placed in a flask with 0.10 M $RuCl_3$ (800 μL, 0.080 mmol) and diluted with H_2O (7.2 mL), CH_3CN (48 mL), and EtOAc (48 mL). Oxone (24.4 g, 40.0 mmol) was added in one portion and stirred until a bright-yellow suspension formed and effervescence ceased. Benzylidene acetophenone (1.66 g, 8.00 mmol) was added in one portion to initially form a brown solution that became yellow over time. The progress of reaction was carefully monitored by TLC (3:1 hexanes:EtOAc), and after 18 min the suspension was diluted with 50 mL EtOAc, and the solid residue filtered off, washing with a further 30 mL EtOAc. The filtrate was washed with 40 mL saturated Na_2SO_3 and 40 mL H_2O. The organic layer was dried over Na_2SO_4 and filtered, and then the solvent was removed under reduced pressure to yield the crude product. Recrystallization from hot EtOH afforded white needle-like crystals that were collected by filtration and washed with cold EtOH followed by Et_2O (0.37 g, 20%). ^{1}H NMR (300 MHz, CD_3CN, 25 °C): δ = 7.99 (d, ^3J(H,H) = 7.2 Hz, 4H; Ar–H), 7.66 (t, ^3J(H,H) = 7.6 Hz, 2H; Ar–H), 7.52 (t, ^3J(H,H) = 7.5 Hz, 4H; Ar–H), 6.34 (d, ^3J(H,H) = 7.2 Hz, 1H; CH), 4.68 (d, ^3J(H,H) = 7.0 Hz, 1H; OH) ppm.

[(6-Ph$_2$TPA)Fe(CH$_3$CN)](ClO$_4$)$_2$ (2-ClO$_4$). $Fe(ClO_4)_2 \cdot 6H_2O$ (0.040 g, 0.11 mmol) was dissolved in CH_3CN (~2 mL) and added to 6-Ph$_2$TPA (0.049 g, 0.11 mmol), and the resulting solution was stirred for 24 h under an N_2 atmosphere. The solution was then concentrated under reduced pressure, and the metal complex was precipitated by introducing excess Et_2O. The solid was then dried under reduced pressure (0.059 g, 73%). Et_2O diffusion into a CH_3CN solution of **2-ClO$_4$** afforded yellow crystals suitable for X-ray crystallography. Anal. calcd for $C_{34}H_{32}Cl_2FeN_6O_8$: C, 52.39; H, 4.14; N, 10.78. Found: C, 52.12; H, 4.25; N, 11.24. μ_{eff} = 5.21 μ_B; UV–vis, nm (ε, M^{-1} cm^{-1}): 285 (14 800); FTIR (KBr, cm^{-1}): 1093 (ν_{ClO4}), 623 (ν_{ClO4}).

[(6-Ph$_2$TPA)Fe(CH$_3$CN)](OTf)$_2$·0.5CH$_2$Cl$_2$ (2-OTf). $Fe(OTf)_2 \cdot 2CH_3CN$ (0.11 mmol) was dissolved in CH_3CN (~2 mL) and added to 6-Ph$_2$TPA (0.11 mmol), and the resulting mixture was stirred for 24 h under a N_2 atmosphere. The solvent was then removed under reduced pressure, and the metal complex precipitated by addition of excess hexanes to a CH_2Cl_2 solution. Anal. calcd for $C_{34}H_{29}F_6FeN_4O_6S_2 \cdot 0.5CH_2Cl_2$: C, 47.07; H, 3.44; N, 7.96. Found: C, 47.04; H, 3.58; N, 7.89. The presence of 0.5 equiv of CH_2Cl_2 in the EA sample was confirmed by integration of the signal of this solvent in the ^{1}H NMR spectrum of the sample. μ_{eff} = 5.03 μ_B; FTIR (KBr, cm^{-1}): 1248 (ν_{OTf}), 1225 (ν_{OTf}), 1167 (ν_{OTf}), 1030 (ν_{OTf}).

[(6-Ph$_2$TPA)Fe(PhC(O)C(OH)C(O)Ph)]ClO$_4$ (3-ClO$_4$). $Me_4NOH \cdot 5H_2O$ (0.0049 g, 0.026 mmol) was dissolved in CH_3CN (2.0 mL) and stirred with 2-hydroxy-1,3-diphenyl-propan-1,3-dione (0.0063 g, 0.026 mmol) for 2 min under a N_2 atmosphere. This solution was then added to a CH_3CN (1.0 mL) solution of **2-ClO$_4$** (0.026 mmol) and stirred for 5 min. The solvent was then immediately removed under reduced pressure. UV–vis, nm (ε, M^{-1} cm^{-1}): 385 (5080). FTIR (KBr, cm^{-1}): 3430 (ν_{OH}), 1094 (ν_{ClO4}), 623 (ν_{ClO4}).

[(6-Ph$_2$TPA)Fe(PhC(O)C(OH)C(O)Ph)]OTf·CH$_2$Cl$_2$ (3-OTf). LiHMDS (0.015 g, 0.091 mmol) was dissolved in Et_2O (~2 mL) and added to a CH_3CN solution of 2-hydroxy-1,3-diphenyl-propan-1,3-dione (0.022 g, 0.090 mmol) under a N_2 atmosphere to form an orange solution that became cloudy after 1 min. To this solution was added a CH_3CN solution of **2-OTf** (0.090 mmol), and the resultant slurry was stirred for 12 h and then filtered through a glass wool/Celite plug. The filtrate was then combined with a second slurry of LiHMDS (0.091 mmol) and 2-hydroxy-1,3-diphenyl-propan-1,3-dione (0.091 mmol) in Et_2O/CH_3CN and stirred for two days. The solvent was removed under reduced pressure, and the crude material was redissolved in CH_2Cl_2 and filtered through a Celite plug. The compound was then precipitated, first by vapor diffusion of Et_2O into a CH_3CN solution, and then by addition of hexanes to a CH_2Cl_2 solution to yield a brown solid (0.062 g, 71%).

Anal. calcd for $C_{47}H_{37}F_3FeN_4O_6S \cdot CH_2Cl_2$: C, 58.08; H, 4.05; N, 5.77. Found: C, 58.03; H, 4.29; N, 5.39. μ_{eff} = 5.13 μ_B; UV–vis, nm (ε, M^{-1}cm^{-1}): 385 (8090); FTIR (KBr, cm^{-1}): 3430 (ν_{OH}), 1256 (ν_{OTf}), 1227 (ν_{OTf}), 1169 (ν_{OTf}), 1032 (ν_{OTf}).

[(6-Ph$_2$TPA)Fe(PhC(O)CHC(O)Ph)]ClO$_4$ (4). $Me_4NOH \cdot 5H_2O$ (0.0067 g, 0.037 mmol) was dissolved in CH_3CN (~2 mL) and stirred with dibenzoylmethane (0.0076 g, 0.034 mmol) for ~1 h under a N_2 atmosphere. This solution was then added to a CH_3CN (~2 mL) solution of **2-ClO$_4$** (0.034 mmol) and stirred for 18 h to produce a dark-red solution. The solvent was then removed under reduced pressure, and the residue was dissolved in CH_2Cl_2 and filtered through a glass wool/Celite plug. The filtrate was condensed under reduced pressure, and precipitation of the product was induced by the addition of excess hexanes. Recrystallization of the crude product from CH_3CN/Et_2O yielded red-brown crystals suitable for X-ray crystallography (0.016 g, 57%). Anal. calcd for $C_{45}H_{37}ClFeN_4O_6$: C, 65.81; H, 4.54; N, 6.83. Found: C, 65.46; H, 4.57; N, 7.27. HRMS (ESI): m/z calcd for $C_{45}H_{37}FeN_4O_2^+$: 721.2266 $[M-ClO_4]^+$; found: 721.2279. μ_{eff} = 5.12 μ_B; UV–vis, nm (ε, M^{-1} cm^{-1}): 357 (13400); FTIR (KBr, cm^{-1}): 1094 (ν_{ClO4}), 623 (ν_{ClO4}).

2,2-Dihydroxy-1,3-diphenylpropan-1,3-dione. Initially this triketone hydrate was prepared by exposing 1,3-diphenylpropantrione to moist air for several weeks, during which time it changed color from yellow to white. The hydrate may also be synthesized by crystallization of 1,3-diphenylpropantrione from wet ethanol. Notably the hydration is reversible, and dehydration will occur over the course of several hours when the hydrate is dissolved in dry solvent. ^{1}H NMR (300 MHz, CD_3CN, 25 °C): δ = 7.98 (d, ^3J(H,H) = 7.2 Hz, 4H; Ar–H), 7.58 (t, ^3J(H,H) = 7.4 Hz, 2H; Ar–H), 7.44 (t, ^3J(H,H) = 7.5 Hz, 4H; Ar–H), 6.03 (s, 2H; OH) ppm. ^{13}C NMR (100.6 MHz, CD_3CN, 25 °C): δ = 196.3, 135.6, 131.3, 130.7, 130.1, 96.8 ppm.

Isomerization of 2-Hydroxy-1,3-diphenyl-propan-1,3-dione Promoted by 2-ClO$_4$. Complex **2-ClO$_4$** (0.010 mmol) was dissolved in ~1 mL CH_3CN, and to this solution was added a CH_3CN solution of 2-hydroxy-1,3-diphenyl-propan-1,3-dione (0.010 mmol) and $Me_4NOH \cdot 5H_2O$ (0.010 mmol) under a N_2 atmosphere. The resulting solution was stirred for 48 h, and the solvent was then removed under reduced pressure. Analysis of the organic products by GC-MS and ^{1}H NMR showed the major product was 2-oxo-2-phenylethylbenzoate.

Reaction of 3-X with O$_2$. A 3.0 mL aliquot of **3-X** (4.8 mM) in CH_3CN or 95% CH_3CN/H_2O was placed in a vial. This solution was then purged with O_2 for 15 s, sealed, and stirred for 12 h. The solvent was then removed under reduced pressure. The organic products were analyzed by LC-MS as described below.

Control Reaction Testing for Benzoylformic Acid Production from 2-Hydroxy-1,3-diphenyl-propan-1,3-dione. $Me_4NOH \cdot 5H_2O$ (0.026 mmol) was dissolved in CH_3CN or 85% CH_3CN/H_2O (1 mL) and was added to 2-hydroxy-1,3-diphenyl-propan-1,3-dione (0.026 mmol). This solution was then either diluted with 2 mL CH_3CN or combined with 0.026 mmol of either $[(6\text{-}Ph_2TPA)Ni(CH_3CN)(H_2O)](ClO_4)_2$ or **2-ClO$_4$** dissolved in CH_3CN (2 mL) and stirred for 5 min. These solutions were then purged with O_2, sealed, and stirred for 12 h. The solvent was then removed under reduced pressure. The organic products were analyzed by LC-MS as described below. Benzoylformic acid was only detected in the reaction involving **2-ClO$_4$**.

Control Reaction Testing for Benzoylformic Production from 1,3-Diphenylpropantrione. Either 1,3-diphenylpropantrione (0.026 mmol) was dissolved in CH_3CN (1 mL) or 2,2-dihydroxy-1,3-diphenylpropan-1,3-dione was dissolved in 85% CH_3CN/H_2O (1 mL). This solution was then either diluted with 2 mL CH_3CN or combined with 0.026 mmol of either $[(6\text{-}Ph_2TPA)Ni(CH_3CN)(H_2O)](ClO_4)_2$ or **2-ClO$_4$** dissolved in CH_3CN (2 mL). To each solution was added 31% H_2O_2 (0.026 mmol) and NEt_3 (0.026 mmol). The solutions were then sealed and stirred for 12 h. The solvent was then removed under reduced pressure. The organic products were analyzed by LC-MS as described below.

Control Reactions Testing for Benzoylformic Production from 2-oxo-2-Phenylethylbenzoate. $Me_4NOH \cdot 5H_2O$ (0.026 mmol) was dissolved in CH_3CN or 85% CH_3CN/H_2O (1 mL) and added to

2-oxo-2-phenylethylbenzoate (0.026 mmol). This solution was then either diluted with 2 mL CH₃CN or combined with **2-ClO₄** (0.026 mmol) dissolved in CH₃CN (2 mL) and stirred for 5 min. These solutions were then purged with O₂, sealed, and stirred for 12 h. The solvent was then removed under reduced pressure. The organic products were then analyzed by LC-MS as described below. Benzoylformic acid was not detected for either of these reactions.

Reaction of 1,3-Diphenylpropantrione with Ferric Salts. Under a nitrogen atmosphere, 1,3-diphenylpropantrione or 2,2-dihydroxy-1,3-diphenylpropan-1,3-dione (0.026 mmol) was dissolved in CH₃CN or 85% CH₃CN/H₂O (1 mL), respectively, and to these solutions was added FeCl₃ or Fe(ClO₄)₃·6H₂O (0.105 mmol) in CH₃CN (2 mL). The solutions were then sealed and stirred for 12 h. The solvent was then removed under reduced pressure. The organic products were then analyzed by LC-MS as described below.

Reaction of 2-Hydroxy-1,3-diphenylpropan-1,3-dione with Fe(ClO₄)₃·6H₂O. Under a nitrogen atmosphere, Me₄NOH·5H₂O (0.026 mmol) was dissolved in 85% CH₃CN/H₂O (1 mL) and added to 2-hydroxy-1,3-diphenyl-propan-1,3-dione (0.026 mmol). To this solution was added Fe(ClO₄)₃·6H₂O (0.105 mmol) in CH₃CN (2 mL). The solution was sealed and stirred for 12 h. The solvent was then removed under reduced pressure. The organic products were then analyzed by LC-MS as described below.

General Procedure for Organic Product Recovery and Analysis. To each crude product mixture, 1 mL of 10 mM HCl and 3 mL Et₂O were added and stirred for 3 h. The organic layer was then decanted, and the aqueous layer extracted with a further 3 mL Et₂O. The organic fractions were combined, and solvent evaporated under reduced pressure. Recovery of the organic material, determined as percent mass of the acireductone or triketone starting material, was typically ~80%. For further analysis, the organic products were redissolved in either CH₃CN (GC-MS) or 1:1 MeOH:H₂O (LC-MS). Products were identified by comparison to the retention times and fragmentation patterns of authentic compounds. The ratio of benzoic acid to benzoylformic acid was determined from a calibration curve based on peak area in the LC-MS spectrum.

¹⁸O Labeling Studies. For H₂¹⁸O labeling, a 3.0 mL aliquot of 4.8 mM **3-ClO₄** in CH₃CN was combined with a 10 μL aliquot of H₂¹⁸O under an nitrogen atmosphere. This solution was then exposed to ¹⁶O₂, sealed, and stirred for 12 h. The solvent was then removed under reduced pressure.

For ¹⁸O₂ labeling, a 3.0 mL aliquot of 4.8 mM **3-ClO₄** was placed in a solvent transfer flask from which the atmosphere was removed by three freeze−pump−thaw cycles. ¹⁸O₂ was then introduced into the flask, after which it was resealed and allowed to stir for 12 h. The solvent was then removed under reduced pressure. ¹⁸O incorporation levels in benzoic acid and benzoylformic acid were determined from the relative intensities of the $[M − 1]^-$, $[M + 1]^-$, and $[M + 3]^-$ molecular ions in the LC-MS spectrum.

■ RESULTS

Complex Synthesis and Characterization. In our initial attempts to generate an iron-containing analogue of **1**, admixture of equimolar amounts of Fe(ClO₄)₂·6H₂O and 6-Ph₂TPA in CH₃CN enabled the facile generation of [(6-Ph₂TPA)Fe(CH₃CN)](ClO₄)₂ (**2-ClO₄**). This compound has been isolated and comprehensively characterized (X-ray crystallography (Figure 1), elemental analysis, ¹H NMR, IR, and a magnetic susceptibility measurement). When **2-ClO₄** is combined with the monoanion of the bulky acireductone in dry acetonitrile, a new complex, [(6-Ph₂TPA)Fe(PhC(O)C(OH)-C(O)Ph)]ClO₄ (**3-ClO₄**) is formed, however it has not been obtained in analytically pure form. Therefore, in an alternative synthetic approach, we combined the anhydrous salt Fe(OTf)₂·2CH₃CN with 6-Ph₂TPA in dry CH₃CN, which led to the facile generation of [(6-Ph₂TPA)Fe(CH₃CN)](OTf)₂ (**2-OTf**). Reaction of this complex with an excess of LiHMDS and acireductone under strictly anhydrous conditions allowed
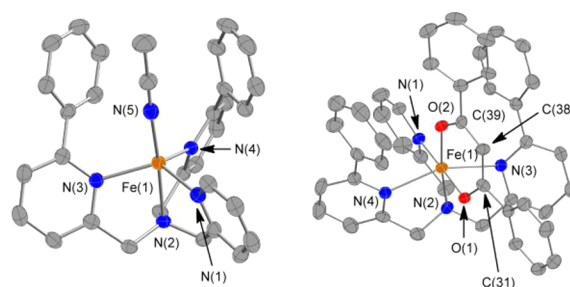

Figure 1. Thermal ellipsoid representation of the cationic portions of **2-ClO₄** (left) and **4** (right). Ellipsoids are drawn at 50% probability. Hydrogen atoms are omitted for clarity.

the generation and isolation of analytically pure [(6-Ph₂TPA)-Fe(PhC(O)C(OH)C(O)Ph)]OTf (**3-OTf**). Thus far X-ray quality crystals of **3-X** (**X = ClO₄** or **OTf**) have not been obtained. Therefore, we have synthesized [(6-Ph₂TPA)Fe-(PhC(O)CHC(O)Ph)]ClO₄ (**4**) by combining **2-ClO₄** with 1 equiv of the anion of dibenzoylmethane, as outlined in Scheme 3, to use as a structural and ¹H NMR spectroscopic

Scheme 3. Synthesis of 2−4[a]
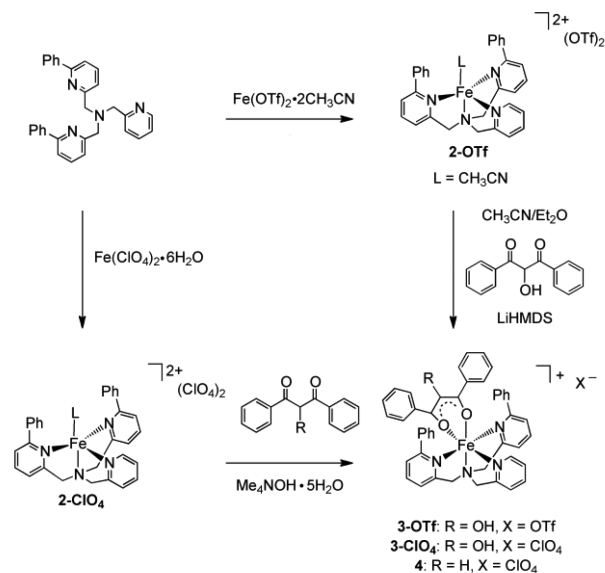
[a] All reactions were performed under anaerobic conditions. CH₃CN was used as the solvent unless otherwise noted.

model to evaluate the coordination mode of the acireductone ligand in **3-X**. X-ray quality crystals of **4** were grown by diffusion of Et₂O into a CH₃CN solution of the complex (see Table 1).

X-ray Crystallography. As shown in Figure 1, X-ray crystallographic studies of **2-ClO₄** revealed a cationic portion containing a single molecule of acetonitrile bound to the iron center, resulting in a trigonal bipyramidal geometry (τ = 0.97).[26] By contrast, **4·0.5CH₃CN** has a cationic portion containing a distorted octahedral Fe(II) center, with the dibenzoylmethane anion coordinated in a bidentate fashion via a six-membered chelate ring. As is expected for the fully delocalized diketonate anion, the C−O bond lengths (O(1)−C(31) 1.278(5) and O(2)−C(39) 1.270(5) Å) are similar, as are the C−C bond lengths within the chelate ring (C(31)−C(38) 1.408(6) and C(38)−C(39) 1.403(6) Å) (see Table 2).

Table 1. Summary of X-ray Data Collection and Refinement[a]

	2-ClO_4	4·0.5CH_3CN
formula	$C_{36}H_{35}Cl_2FeN_7O_8$	$C_{90}H_{74}Cl_2Fe_2N_8O_{12}·CH_3CN$
M_r	820.46	1683.23
crystal system	monoclinic	tetragonal
space group	$P2_1/c$	I-4
a, Å	13.7317(3)	34.4839(4)
b, Å	19.1640(3)	34.4839(4)
c, Å	14.2994(4)	13.5578(2)
α, °	90	90
β, °	94.5399(10)	90
γ, °	90	90
V, Å^3	3751.14(15)	16122.1(4)
Z	4	8
D_c, Mg m^{-3}	1.453	1.387
T, K	150(1)	150(1)
color	yellow	red-brown
crystal shape	prism	plate
crystal size, mm	0.28 × 0.23 × 0.15	0.35 × 0.35 × 0.05
μ, mm^{-1}	0.606	0.497
F(000)	1696	6992
θ range, °	3.75−27.48	2.00−26.00
completeness to θ, %	99.2	99.3
reflections collected	15 757	13 636
independent reflections	8519	13 631
R_{int}	0.0365	0.0525
data/restraints/ parameters	8519/0/595	13631/0/1057
GoF; F^2	1.022	1.012
R_1, wR_2; $I > 2\sigma(I)$	0.0542, 0.1379	0.0515, 0.0914
R_1, wR_2; all data	0.0811, 0.1569	0.0817, 0.1028
max/min transmission	0.9146/0.8487	0.9756/0.8454
$\Delta\rho_{max/min}$, eÅ^{-3}	0.696/−0.594	0.701/−0.395

[a]Radiation used: Mo Kα (λ = 0.71073 Å); diffractometer: Nonius KappaCCD.

Table 2. Selected Bond Distances (Å) and Angles (°) for 2-ClO_4 and 4·0.5CH_3CN

2-ClO_4

Fe(1)−N(1)	2.090(2)	N(1)−Fe(1)−N(2)	78.81(9)
Fe(1)−N(2)	2.190(2)	N(1)−Fe(1)−N(3)	123.11(9)
Fe(1)−N(3)	2.149(2)	N(5)−Fe(1)−N(2)	172.11(9)
Fe(1)−N(4)	2.123(2)	N(4)−Fe(1)−N(3)	113.93(9)
Fe(1)−N(5)	2.096(2)	N(5)−Fe(1)−N(3)	100.93(9)
N(1)−Fe(1)−N(4)	108.19(9)	N(5)−Fe(1)−N(4)	111.60(9)
N(1)−Fe(1)−N(5)	97.13(9)	N(4)−Fe(1)−N(2)	76.21(8)
N(3)−Fe(1)−N(2)	76.11(9)		

4·0.5CH_3CN[a]

Fe(1)−N(1)	2.156(3)	O(2)−Fe(1)−N(2)	169.06(13)
Fe(1)−N(2)	2.194(3)	O(1)−Fe(1)−N(2)	94.92(12)
Fe(1)−N(3)	2.371(4)	N(1)−Fe(1)−N(2)	78.70(13)
Fe(1)−N(4)	2.293(4)	O(2)−Fe(1)−N(4)	111.32(13)
Fe(1)−O(1)	2.012(3)	O(1)−Fe(1)−N(4)	95.81(13)
Fe(1)−O(2)	1.979(3)	N(1)−Fe(1)−N(4)	79.61(13)
O(1)−C(31)	1.278(5)	N(2)−Fe(1)−N(4)	78.59(14)
O(2)−C(39)	1.270(5)	O(2)−Fe(1)−N(3)	96.72(12)
O(2)−Fe(1)−O(1)	88.82(12)	O(1)−Fe(1)−N(3)	86.26(12)
O(2)−Fe(1)−N(1)	98.08(12)	N(1)−Fe(1)−N(3)	95.13(12)
O(1)−Fe(1)−N(1)	172.73(13)	N(2)−Fe(1)−N(3)	73.32(13)

[a]Data for one of two cations present in asymmetric unit.

Figure 2. Comparison of selected paramagnetically shifted features of 2−4.
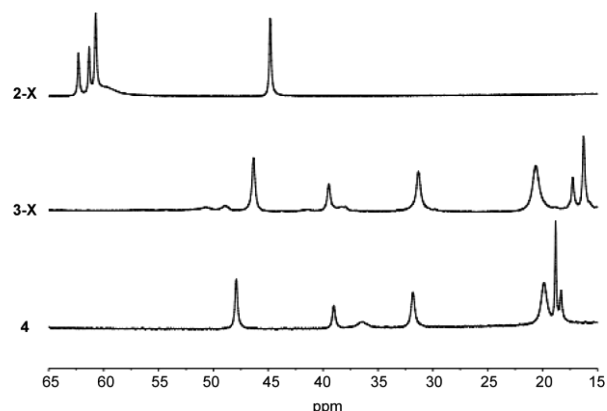
The overall structural features of **4·0.5CH_3CN**, as well as the bond distances involving the coordinated diketonate anion, are highly similar to those found for the Ni(II)-containing acireductone complex **1**.[12]

^{1}H NMR Spectroscopy. A previous study on the paramagnetically shifted features in the ^{1}H NMR spectra for a variety of nickel complexes with the same chelate ligand (6-Ph$_2$TPA) has demonstrated the sensitivity of the peak distribution pattern to the coordination of different anions.[22] As shown in Figure 2, complex **3-ClO$_4$** exhibits signals in the paramagnetically shifted region of the ^{1}H NMR spectrum that are very similar to those exhibited by the dibenzoylmethane complex **4**, albeit the signals for **3-ClO$_4$** are shifted slightly upfield.[27] By contrast, the solvate complex **2-ClO$_4$** has a distinctly different pattern of peaks in the paramagnetic region. It is also worth noting that **2-OTf** and **3-OTf** have the same peak distribution patterns as **2-ClO$_4$** and **3-ClO$_4$**, respectively. On the basis of these spectroscopic comparisons, we formulate the solution structure of **3-X** as [(6-Ph$_2$TPA)Fe(PhC(O)-C(OH)C(O)Ph)]X, wherein similar to the Ni(II)-analog **1**, the bulky acireductone is bound via a six-membered chelate ring. We note that chemical shifts of ^{1}H NMR resonances of **2-OTf**, **2-ClO$_4$**, **3-OTf**, and **4** are available in Table S1.

UV−vis and Infrared Spectroscopy. The absorption spectra of **3-ClO$_4$** and **3-OTf** exhibit features with λ_{max} = 385 nm, albeit with differing extinction coefficients depending on the counterion (5080 and 8090 M^{-1} cm^{-1}, respectively). We attribute this absorption band primarily to a $\pi−\pi^*$ transition of the acireductone diketonate that is coordinated to the iron center, consistent with our structural proposal of the acireductone being bound via a six-membered chelate ring. Similar features are found for both **4** (λ_{max} = 357 nm; hypsochromically shifted, as expected in the absence of the hydroxyl group) and **1** (λ_{max} = 399 nm) when dissolved in acetonitrile (Figure S1).[12] We note that a shoulder feature on the longer wavelength side of the $\pi−\pi^*$ transition of **3-X** and **4** may be due to an MLCT transition, as has been identified in spectroscopic studies of Dke1 and relevant model compounds.[28,29]

The proposed six-membered chelate is additionally supported by the IR spectral features of **3-X**, wherein a O−H stretch is present at ∼3430 cm^{-1}, and no free C═O stretch is found at ∼1700 cm^{-1}. If the acireductone were coordinated as a

five-membered ring, the hydroxyl group would instead likely be deprotonated and a free C=O moiety would be present.

Thus, in contrast to the proposed binding mode of the acireductone in the enzyme–substrate complex, wherein changing the metal center from Ni to Fe changes the binding mode of the acireductone from a six-membered to a five-membered chelate ring, in our synthetic systems, our acireductone binds via a six-membered chelate when either metal ion is present. This is unsurprising, as the difference in Lewis acidity between Ni(II) and Fe(II) is modest and is not proposed as the factor that differentiates the binding mode in the enzyme. It is, rather, changes in the tertiary structure of the enzyme, resulting in a more open binding pocket in Fe-ARD′ that are proposed to direct the acireductone to bind via a five-membered chelate.[30] Our model systems have the same secondary structural features, as defined by having the same 6-Ph₂TPA chelate ligand, and thus exhibit the same binding mode for the acireductone. Therefore, our model system is an ideal case to test the chelate hypothesis for the differing reactivity of Fe-ARD′ and Ni-ARD; if the proposal is correct, our iron-containing complexes **3-X** should exhibit the same dioxygenase reactivity as our previously reported nickel-containing system **1**.

Anaerobic Reactivity. Our inability to generate analytically pure **3-ClO₄** has been due to an anaerobic water-promoted isomerization reaction of the acireductone ligand. The exclusion of water in the synthesis of **3-OTf** was likely the factor that allowed its generation in analytically pure form. Evidence for the formation of **3-ClO₄**, followed by its subsequent decay, was found by monitoring (UV–vis) of a reaction mixture, wherein an acetonitrile solution of **2-ClO₄** was combined with the bulky acireductone anion under anaerobic conditions. Slow decay of the 385 nm absorption band was observed upon prolonged stirring, and analysis of the organic products by GC-MS showed that the ester 2-oxo-2-phenylethylbenzoate, an isomer of the bulky acireductone, had been produced. This same isomerization reactivity has been previously reported for the Co(II) analog [(6-Ph₂TPA)Co(PhC(O)C(OH)C(O)Ph)]ClO₄ (**5**), wherein a water and Lewis acid-mediated isomerization reaction of the acireductone ligand resulted in the formation of the same ester (2-oxo-2-phenylethylbenzoate, Scheme 4).[21] By contrast, the

Scheme 4. Proposed Mechanism for the Isomerization of 2-Hydroxy-1,3-diphenyl-propan-1,3-dione To Form 2-Oxo-2-phenylethylbenzoate
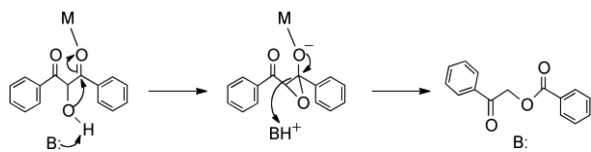
nickel-containing complex **1** does not efficiently promote this isomerization chemistry under wet conditions. We also note that in the O₂ reactivity studies of **3-ClO₄** described below, the reaction to generate ester is always operative.

Aerobic Reactivity. Exposure of acetonitrile solutions of **3-X** to O₂ at ambient temperature results in the rapid bleaching of the 385 nm absorption feature (Figure 3), indicating decomposition of the acireductone anion. Analysis of the headspace gas of the reaction vessel shows that CO has been produced qualitatively. After prolonged exposure to O₂, total loss of the well-defined paramagnetically shifted features in the ¹H NMR spectrum is observed, consistent with a change in
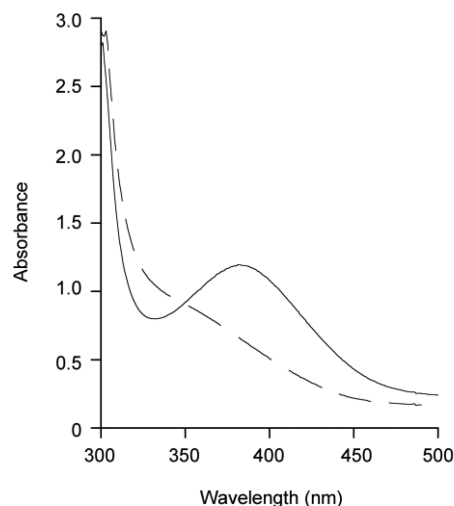

Figure 3. UV–vis spectra of **3-ClO₄** before (solid line) and after (dashed line) the addition of O₂.

oxidation state from Fe(II) to Fe(III). Our attempts to isolate and characterize the iron-containing products of these oxygenation reactions have thus far been unsuccessful, presumably due to the poor affinity of Fe(III), a hard Lewis acid, for the aryl-appended TPA ligand. However, acidification of the crude reaction mixture followed by extraction with Et₂O has allowed us to analyze the organic compounds produced in the decomposition of the acireductone. In the reaction of **3-OTf** with O₂, the major products observed were benzoic acid and benzil, along with small amounts of the ester. These products were the same as were observed in the reaction of the Ni analogue **1** with O₂[20] and thus are generally consistent with the chelate hypothesis, which predicts that **3-OTf** and **1**, having the same six-membered chelate ring for acireductone binding, should produce the same products in a dioxygenase reaction.

It was therefore very surprising to discover that benzoyl-formic acid is produced in the reaction of **3-ClO₄** with O₂, in addition to the other products produced in the reaction of **3-OTf** (Scheme 5; Figure S2). Benzoylformic acid is an α-keto

Scheme 5. Organic Products Detected in the Reaction of 3-X with O₂ in CH₃CN[a]
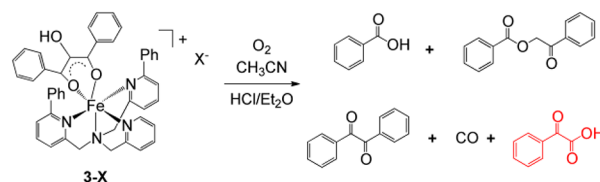
[a]Benzoylformic acid (red) was only detected when X = ClO₄.

acid and is the expected product in the oxidation of the bulky acireductone if it were undergoing Fe-ARD′-type reactivity. Given that all our spectroscopy detailed above strongly suggests that **3-OTf** and **3-ClO₄** have the same solution structure, precluding a five-membered chelate, this change in reactivity was very interesting. Our initial hypothesis was that the ester initially formed by an isomerization reaction could undergo a separate oxygenation reaction to generate benzoyl-2-oxo-2-phenylethanoate. This anhydride would subsequently undergo hydrolysis to generate the observed benzoylformic acid (and an equivalent of benzoic acid, Scheme S1). However, a control

reaction in which the ester was exposed to O_2 in the presence of **2-ClO$_4$** did not lead to the generation of benzoylformic acid. Rather only trace amounts of the hydrolytic products benzoic acid and 2-hydroxyacetophenone were detected in addition to unreacted ester.
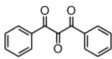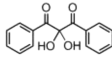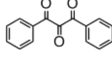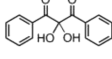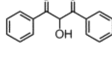
Kinetics. In order to gain more insight into why **3-ClO$_4$** exhibits different regioselectivity in C−C bond cleavage than **1** and **3-OTf**, we undertook mechanistic studies. For both **3-ClO$_4$** and **3-OTf**, the reaction is found to be first order in each of **3-X** and O_2, with an overall rate constant, $k_2 = 0.40$ M^{-1} s^{-1} (Figures S3 and S4). The similarity of the rate in each case implies they have the same rate-determining step, and the differentiation in terms of reactivity likely occurs after the acireductone itself has been consumed. It is also worth noting that these reactions are slightly slower than was observed in the analogous reaction of **1** ($k = 1.7$ M^{-1} s^{-1}).[13]

Investigations of Fe/O$_2$ Reactivity. A common paradigm in dioxygenase reactions involving a ferrous center is the direct metal-centered activation of O_2, forming a ferric-superoxo species. Speculating that such a species could be partially responsible for the differentiation in reactivity between **1** and **3-ClO$_4$**, we investigated its feasibility. The formation of such a species would require the dissociation of one of the phenyl-appended pyridyl arms of the chelate ligand to open up a coordination position. Low-temperature ^{1}H NMR studies of **4** in CD$_3$CN (−40 °C) and CD$_3$OD (−70 °C) have shown no evidence of loss of the C_s symmetry of the complex, suggesting that dissociation of a chelate ligand arm is unlikely to be occurring. Additionally, in the reaction of **3-X** with O_2 in acetonitrile at −40 °C, we have observed no intermediates consistent with the formation of a ferric-superoxo species by UV−vis. Attempts to intercept a superoxo intermediate by hydrogen atom abstraction from common probes, such as dihydroanthracene, 2,4-di^{t}butylphenol and 2,4,6-tri^{t}butylphenol have all yielded a negative result.[31] Based on these results we conclude that it is unlikely that the reaction proceeds via a ferric-superoxo intermediate.

Isotopic Labeling. Labeling studies of the reaction of **3-ClO$_4$** with $^{18}O_2$ show a modest incorporation of a single label into both benzoic acid (36%) and benzoylformic acid (53%). We hypothesized that water in the reaction mixture (due to the use of the pentahydrate base Me$_4$NOH·5H$_2$O to generate **3-ClO$_4$**) was at least partially responsible for the loss of label, as addition of H$_2$^{18}O to the $^{16}O_2$ reaction results in modest label incorporation (Scheme S3). To probe whether water could have a role in the reaction, we repeated the reaction of **3-OTf** with O_2 in the presence of 5% added water. Gratifyingly, we observed the production of benzoylformic acid (Table 3), therefore indicating that the presence of water had been the reason for the differing observed reactivities of **3-OTf** and **3-ClO$_4$**.

Scope of α-Keto Acid Formation. Having established the importance of water in the generation of the α-keto acid, we conducted a series of control reactions specifically searching for benzoylformic acid formation. Most importantly, we have reinvestigated the products generated in the reaction of the nickel complex **1** with O_2 in both pure CH$_3$CN and 95% CH$_3$CN/H$_2$O using the workup procedure and analysis methods (GC-MS and LC-MS) employed for the O_2 reaction of **3-X**. Notably, no benzoylformic acid formation was detected starting from **1** (Scheme S2 and Figure S2 (LC-MS)). Additionally, reaction of the triketone (1,3-diphenylpropantrione) in the presence of the hydroperoxide anion and [(6-Ph$_2$TPA)Ni-(CH$_3$CN)(H$_2$O)](ClO$_4$)$_2$ resulted in no detectable benzoylformic

Table 3. Summary of Production of Benzoylformic Acid

| Reaction		Solvent	Benzoic acid[a]	Benzoylformic acid[a]
3-OTf	O_2 →	CH$_3$CN	100	0
3-ClO$_4$	O_2 →	CH$_3$CN	82	18
3-OTf	O_2 →	95% CH$_3$CN/H$_2$O	81	19
3-OTf	O_2 →	50% CH$_3$CN/H$_2$O	64	36
(structure) **2-ClO$_4$**	HO$_2^{-}$[b] →	CH$_3$CN	83	17
(structure) **2-ClO$_4$**	HO$_2^{-}$[b] →	95% CH$_3$CN/H$_2$O	73	27
(structure)	2 FeCl$_3$ →	CH$_3$CN	100	0
(structure)	2 Fe(ClO$_4$)$_3$·6H$_2$O →	95% CH$_3$CN/H$_2$O	61	39
(structure)	Me$_4$NOH·5H$_2$O / 4 Fe(ClO$_4$)$_3$·6H$_2$O →	95% CH$_3$CN/H$_2$O	67	33

[a]Relative percentage of the total amount of benzoic acid and benzoylformic acid determined by LCMS peak area. Benzil and ester are additional products not presented in this table. [b]HO$_2^{-}$ generated in situ by combining 1.1 equivalents of 30% H$_2$O$_2$ $_{(aq)}$ and NEt$_3$.

acid formation (Scheme S2). Treatment of the tetramethylammonium salt of the bulky acireductone anion with O_2 also failed to yield any α-keto acid formation. Taken together, these results imply that both water and an iron center are required for α-keto acid formation.

Raising the amount of water present in the reaction of **3-OTf** with O_2 results in a marked increase in the amount of benzoylformic acid produced, as summarized in Table 3. However, we have been unable to generate equimolar amounts of benzoic acid and benzoylformic acid regardless of the amount of water present in the system. Interestingly, reaction of the triketone (the two-electron oxidized form of the acireductone) with HO$_2^{-}$ in the presence of a ferrous complex also results in the generation of benzoylformic acid. When the same reaction is repeated, starting from the hydrated triketone (2,2-dihydroxy-1,3-diphenylpropan-1,3-dione) an increase in the amount of benzoylformic acid produced is observed (Table 3). These results suggest that the water sensitivity of the oxidation chemistry is due to the hydration of a triketone intermediate.

We have also investigated the role of ferric species in the reaction chemistry. Attempts to isolate ferric complexes by the combination of Fe(ClO$_4$)$_3$·6H$_2$O, 6-Ph$_2$TPA, Me$_4$NOH·5H$_2$O, and the bulky acireductone have been unsuccessful. Monitoring these reactions by ^{1}H NMR in the paramagnetic region shows the growth of peaks consistent with the reduction of Fe^{III} to form the ferrous species **2-ClO$_4$** (Figure S5). Subsequent analysis of the organic products of this reaction shows the production of the ester as a major species as well as triketone and trace amounts of benzoic acid (Scheme 6). Given that ferric/ferrous couple is a one-electron process, we next combined 4 equiv of a ferric salt with the acireductone anion or 2 equiv with the triketone. As shown in Table 3, these reactions also lead to carbon−carbon bond cleavage, with the regioselectivity influenced by the water content of the reaction mixture. We note that the ferric-mediated oxidative cleavage of vicinal triketones in water has previously been reported,[32] and the oxidation of acireductone analogues, such as ascorbic acid by ferric ions, is well documented.[33,34] This oxidation of an

Scheme 6. Attempted Synthesis of [[(6-Ph$_2$TPA)Fe-(PhC(O)C(OH)C(O)Ph)](ClO$_4$)$_2$, and the Resulting Products Including Oxidized Organic Species
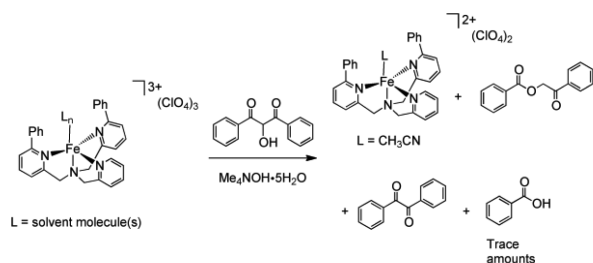
acireductone in the absence of molecular oxygen is particularly interesting due to the recent discovery of the operation of a methionine salvage pathway under anaerobic conditions.[35]

■ DISCUSSION

The chelate ring hypothesis was formulated on the basis of a number of observations in studies of Ni-ARD and Fe-ARD'.[9] First, oxygen uptake studies, as well as spectroscopic studies performed in the presence of oxygen, provided no evidence for oxygen binding at the active site in either metal-containing form of the enzyme. Additionally, Fe-ARD'-type reactivity was found to occur when the enzyme is reconstituted with magnesium, implying that iron-centered redox activity may not be important in directing the regiospecificity of the reaction. Second, NMR studies provided evidence for a metal-dependent entropy switch that converts the active site tertiary structure between a closed (Ni-ARD) and open (Fe-ARD') form. Docking studies show that the acireductone would likely coordinate via a five-membered chelate in Fe-ARD', but in the more congested Ni-ARD active site, it would bind via a less sterically demanding six-membered chelate.[30] These binding modes would activate the C(1)/C(2) or C(1)/C(3) positions, respectively, for reaction with oxygen (Scheme 1), leading in turn to the proposed products for the Fe-ARD' and Ni-ARD catalyzed reactions. Notably, the structural data currently available for enzyme–substrate (ES) adducts of Fe-ARD' or Ni-ARD, respectively, are limited to XAS data, which does not provide definitive proof of the substrate coordination motif.[9] Additionally, the UV–vis absorption features of the ES adducts are similar, which may actually indicate that there is no difference in binding mode.

Our previous studies of a nickel-containing complex (1) supported the chelate hypothesis in terms of the coordination mode of the bulky acireductone ligand, which is akin to that proposed for the ES complex of Ni-ARD. The O$_2$ reactivity of 1, while resulting in the formation of Ni-ARD type products, proceeded via a different pathway than that being proposed for the enzyme. Specifically, the initial reaction in the model system leads to the formation of triketone and hydroperoxide intermediates from which carbon–carbon bond cleavage was found to occur. In the enzyme, the coordinated acireductone is proposed to react directly with O$_2$ to give a coordinated cyclic peroxide species from which aliphatic C–C bond cleavage occurs. The results described herein show that a simple change in the metal ion from Ni(II) in 1 to Fe(II) in 3-X, while maintaining the same supporting ligand coordination environment, has no effect on the coordination mode of the bulky acireductone. However, despite the congruence of the structure of 1 and 3-X, α-keto acid formation was found to occur upon reaction of 3-X with O$_2$ in the presence of water. Thus, an

oxidative pathway is accessible, leading to a change in the regiospecificity of carbon–carbon bond cleavage that does not require distinct acireductone coordination motifs, in contrast to the chelate hypothesis.

In the reaction of 3-X with O$_2$ in the presence of water we never observe the formation of benzoic acid and benzoylformic acid in an equimolar ratio (Table 3). Thus, there are always at least two oxidative pathways operative. Regardless of conditions, it appears that an O$_2$ reaction akin to that found for 1 is always operative in the Fe(II)-containing system. This reaction leads to the formation of 2 equiv of benzoic acid and carbon monoxide. When water is added, a new reaction pathway is enabled, wherein 1 equiv each of benzoic acid and benzoylformic acid are generated. Because complex 1 exhibits only the first type of reactivity, comparative studies of the reactivity of 1 and 3-X enable us to probe for the chemical factors that enable α-keto acid formation. From these studies we find that regardless of metal ion or water content of the system, the initial step is the two-electron oxidation of the acireductone by dioxygen to form a triketone and the hydroperoxide anion as intermediates. This proposal is supported by our previous mechanistic studies of the O$_2$ reaction of 1 as well as kinetic studies that show a similar rate-determining step for the oxidation of 1 and 3-X in the presence or absence of water. The involvement of triketone and hydroperoxide intermediates is also supported by studies involving authentic triketone and hydrogen peroxide in the presence of the corresponding [(6-Ph$_2$TPA)M(CH$_3$CN)$_x$]$^{2+}$ (M = Ni (x = 2) or Fe (x = 1)) complex. In these reactions we observed similar regioselectivity, as in the reaction of 1 or 3-X, indicating that it is at the triketone level that a differentiation in the chemistry occurs.

In the absence of water, the triketone intermediate formed in the O$_2$ reactions of 1 and 3-X will undergo reaction with the hydroperoxide anion to selectively cleave the C(1)−C(2) and C(2)−C(3) bonds and release CO. This chemistry is consistent with that previously reported by Pochapsky, wherein 2,3,4-pentanetrione was shown to undergo reaction with H$_2$O$_2$ to give 2 equiv of acetic acid and carbon monoxide.[36] For 3-X in the presence of water, we propose that an additional reaction pathway is operative due to hydration of the triketone intermediate. Triketone hydration is a well-known process, and the central carbonyl of 1,3-diphenyltriketone is the most electrophilic and therefore will be the site of initial hydration.[37] Once formed, we propose that the hydrated triketone may interact with the iron center to form a five-membered chelate ring (Scheme 7),

Scheme 7. Proposed Reaction Pathway Involving Triketone Hydration As a Means To Generate Fe-ARD'-Type Products Containing Oxygen Atoms Derived From O$_2$
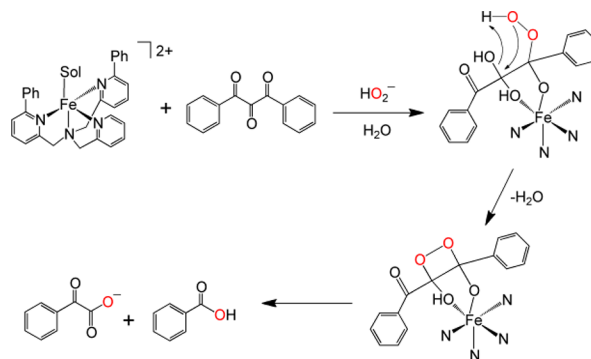
which becomes susceptible to attack by hydroperoxide at an activated terminal carbonyl moiety. Formation of a four-membered dioxetane ring via loss of water would generate the species from which $C(1)-C(2)$ bond cleavage and α-ketoacid formation could occur.

The reaction pathway outlined in Scheme 7 shows that it is the hydration and subsequent coordination of an intermediate, not differences in chelation involving the acireductone substrate itself (chelate hypothesis), that determine the regioselectivity of the reaction. This is in contrast to the reaction pathways of other metal-containing dioxygenases and their model systems, wherein changes in the primary and/or secondary environment of the metal center determine the regioselectivity of carbon–carbon bond cleavage.[38] In terms of ARD enzymes, it is important to note that the active site in Fe-ARD′ is much more open and thus solvent-exposed when compared to the Ni-ARD active site, wherein a tryptophan loop maintains a hydrophobic microenvironment.[30] The reaction pathway shown in Scheme 7 provides a means for ^{18}O incorporation from $^{18}O_2$ in the α-ketoacid product. The substoichiometric ^{18}O incorporation that is found in the α-keto acid generated in the O_2 reaction of **3-X** (∼50%) and in the dioxygenase reactivity of Fe-ARD′ (∼78%)[39] suggests that water exchange may be important for both the model system and the enzyme. The involvement of a triketone-type intermediate in the enzymatic system cannot currently be ruled out on the basis of either experimental or computational studies. Therefore, our future work will involve approaches toward examining the feasibility of a triketone-type pathway in reactions involving $C(1)-$H-containing ARD substrates. We note that recent advances in the synthesis of $C(1)-$H triketones will be instrumental in carrying out this work.[40]

Of course the question then arises as to why the $C(1)-C(2)$ cleavage pathway leading to α-keto acid formation is not operative for the nickel-containing complex **1**. Our working hypothesis is that the Ni(II) center does not effectively mediate the hydration of the triketone intermediate, preventing this species from forming in significant amounts during the reaction progression. This hypothesis is supported by the differing anaerobic, water-dependent bulky acireductone isomerization chemistry of the nickel and iron complexes **1** and **3-X**. While **1** does not undergo isomerization of the acireductone, **3-X** undergoes rapid isomerization in the presence of water (Scheme 4). Similar water-dependent isomerization of the acireductone to the ester, as well as subsequent hydrolysis, was also observed in solutions containing the cobalt complex **5**. Interestingly, the solid-state structures of the solvate complexes $[(6\text{-Ph}_2\text{TPA})\text{M}-(\text{CH}_3\text{CN})_x]^{2+}$ are pentacoordinate, with a single solvent molecule when M = Fe or Co but hexacoordinate with two solvent molecules when M = Ni.[19] The differing coordination preferences for the metal ions in these systems may be responsible for the differences in Lewis acid activation for the triketone and/or water that would influence the formation of hydrated triketone and acireductone isomerization.

We note that an alternative route for α-keto acid formation could involve the direct oxidation a hydrated triketone by ferric ions generated in solution (Scheme 8). In this regard, it would be expected that ferric ions could rapidly promote hydration of the triketone, and previous studies have demonstrated ferric-mediated oxidative cleavage of vicinal triketones in aqueous solutions to give α-keto acid and carboxylic acid products.[32] While this type of reactivity is certainly viable in our systems, it would not explain the observed isotope incorporation data,

Scheme 8. Proposed Sequence for Hydrated Triketone Aliphatic Carbon–Carbon Bond Cleavage Promoted by Ferric Iron Species
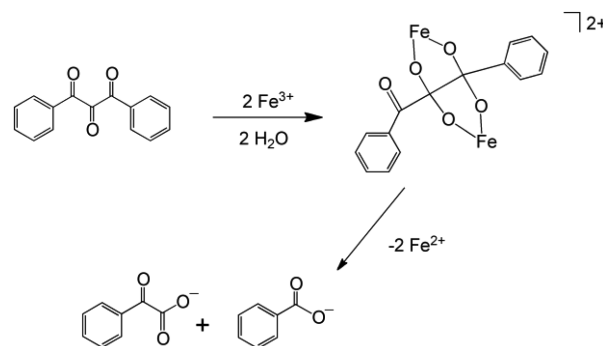
wherein ^{18}O from $^{18}O_2$ is incorporated into the α-keto acid product.[41] In this regard, our studies do not exclude a pathway, wherein the HO_2^- produced in the reaction of **3-X** with O_2 first oxidizes Fe(II) to Fe(III), which then acts as Lewis acid to mediate triketone hydration. The hydrated triketone could then react with an additional equivalent of HO_2^- to give Fe-ARD′ type products, wherein the ^{18}O label from $^{18}O_2$ would be incorporated.

■ CONCLUSION

The chelate hypothesis had remained unchallenged in the literature to date as an explanation for the differing regiospecificity of Ni-ARD and Fe-ARD′ without the need to invoke metal-centered redox chemistry, which has not been observed in the native enzymes. In this first study of an iron-containing model system, designed to directly probe this hypothesis, we have found that the chelate hypothesis is not necessary to explain the differentiation in reactivity. Rather, in our model system, a difference between nickel and iron in the hydration of a triketone intermediate allows a change in regioselectivity of the reaction. This is an alternative proposition for the Fe-ARD′ reaction, as it would be accounted for by the differences in solvent accessibility in the active sites of Ni-ARD and Fe-ARD′ without a need to dismiss the similarity in absorption spectra for the enzyme–substrate adducts. The notion of hydration of an intermediate as the key factor differentiating regioselectivity also provides a potential framework for understanding how oxidation of an acireductone may occur in anaerobic systems using oxidants other than dioxygen.

■ ASSOCIATED CONTENT

Ⓢ Supporting Information

Crystallographic files in CIF format; table of chemical shifts of ^{1}H NMR resonances for Fe(II) compounds; LC-MS data for organic products of reactions of **1** and **3** with O_2; schemes describing control reactions and ^{18}O-labeling studies. This material is available free of charge via the Internet at http://pubs.acs.org.

■ AUTHOR INFORMATION

Corresponding Author

lisa.berreau@usu.edu

Notes

The authors declare no competing financial interest.

REFERENCES

(1) Lange, S. J.; Que, L., Jr. *Curr. Opin. Chem. Biol.* **1998**, *2*, 159−172.

(2) Bugg, T. D. H.; Ramaswamy, S. *Curr. Opin. Chem. Biol.* **2008**, *12*, 134−140.

(3) Broderick, J. B. *Essays Biochem.* **1999**, *34*, 173−189.

(4) Straganz, G. D.; Glieder, A.; Brecker, L.; Ribbons, D. W.; Steiner, W. *Biochem. J.* **2003**, *369*, 573−581.

(5) Hopper, D. J.; Kaderbhai, M. A. *Biochem. J.* **1999**, *344*, 397−402.

(6) Cicchillo, R. M.; Zhang, H.; Blodgett, J. A.; Whitteck, J. T.; Li, G.; Nair, S. K.; van der Donk, W. A.; Metcalf, W. W. *Nature* **2009**, *459*, 871−874.

(7) Wray, J. W.; Abeles, R. H. *J. Biol. Chem.* **1993**, *268*, 21466−21469.

(8) Albers, E. *IUBMB Life* **2009**, *61*, 1132−1142.

(9) Pochapsky, T. C.; Ju, T.; Dang, M.; Beaulieu, R.; Pagani, G. M.; OuYang, B. In *Metal Ions in Life Sciences*; Sigel, A., Sigel, H., Sigel, R. K. O., Eds.; Wiley-VCH: Weinheim, Germany, 2007; Vol. 2, pp 473−500.

(10) Dai, Y.; Wensink, P. C.; Abeles, R. H. *J. Biol. Chem.* **1999**, *274*, 1193−1195.

(11) Motterlini, R.; Otterbein, L. E. *Nat. Rev. Drug Discov.* **2010**, *9*, 728−743.

(12) Szajna, E.; Arif, A. M.; Berreau, L. M. *J. Am. Chem. Soc.* **2005**, *127*, 17186−17187.

(13) Berreau, L. M.; Borowski, T.; Grubel, K.; Allpress, C. J.; Wikstrom, J. P.; Germain, M. E.; Rybak-Akimova, E. L.; Tierney, D. L. *Inorg. Chem.* **2011**, *50*, 1047−1057.

(14) Roberts, J. D.; Smith, D. R.; Lee, C. C. *J. Am. Chem. Soc.* **1951**, *73*, 618−625.

(15) Armarego, W. L. F.; Perrin, D. D. *Purification of Laboratory Chemicals*, 4th ed.; Butterworth−Heinemann, Boston, MA, 1996.

(16) Hagen, K. S. *Inorg. Chem.* **2000**, *39*, 5867−5869.

(17) So, J.-H.; Boudjouk, P. *Inorg. Chem.* **1990**, *29*, 1592−1593.

(18) Plietker, B. *J. Org. Chem.* **2003**, *68*, 7123−7125.

(19) Makowska-Grzyska, M. M.; Szajna, E.; Shipley, C.; Arif, A. M.; Mitchell, M. H.; Halfen, J. A.; Berreau, L. M. *Inorg. Chem.* **2003**, *43*, 7472−7488.

(20) Szajna-Fuller, E.; Rudzka, K.; Arif, A. M.; Berreau, L. M. *Inorg. Chem.* **2007**, *46*, 5499−5507.

(21) Grubel, K.; Ingle, G. K.; Fuller, A. L.; Arif, A. M.; Berreau, L. M. *Dalton Trans.* **2011**, *40*, 10609−10620.

(22) Szajna, E.; Dobrowolski, P.; Fuller, A. L.; Arif, A. M.; Berreau, L. M. *Inorg. Chem.* **2004**, *43*, 3988−3997.

(23) Evans, D. F. *J. Chem. Soc.* **1959**, 2003−2005.

(24) Achord, J. M.; Hussey, C. L. *Anal. Chem.* **1980**, *52*, 601−602.

(25) Wolsey, W. C. *J. Chem. Educ.* **1973**, *50*, A335−A337.

(26) Addison, A. W.; Rao, T. N.; Reedijk, J.; van Rijn, J.; Vershcoor, G. C. *J. Chem. Soc., Dalton Trans.* **1984**, 2177−2184.

(27) X-ray crystallographically-characterized Ni(II) bulky acireductone complex **1** and its dibenzoylmethane analog, [(6-Ph$_2$TPA)Ni(PhC(O)CHC(O)Ph)]ClO$_4$, exhibited a similar ^{1}H NMR spectral congruence.[20]

(28) (a) Park, H.; Baus, J. S.; Lindeman, S. V.; Fiedler, A. T. *Inorg. Chem.* **2011**, *50*, 11978−11989. (b) Park, H.; Bittner, M. M.; Baus, J. S.; Lindeman, S. V.; Fiedler, A. J. *Inorg. Chem.* **2012**, *51*, 10279−10289.

(29) Diebold, A. R.; Neidig, M. L.; Moran, G. R.; Straganz, G. D.; Solomon, E. I. *Biochemistry* **2010**, *49*, 6945−6952.

(30) Ju, T.; Goldsmith, R. B.; Chai, S. C.; Maroney, M. J.; Pochapsky, S. S.; Pochapsky, T. C. *J. Mol. Biol.* **2006**, *363*, 823−834.

(31) Mukherjee, A.; Cranswick, M. A.; Chakrabarti, M.; Paine, T. K.; Fujisawa, K.; Münck, E.; Que, L., Jr. *Inorg. Chem.* **2010**, *49*, 3618−3628.

(32) Mecinović, J.; Hamed, R. B.; Schofield, C. J. *Angew. Chem., Int. Ed. Engl.* **2009**, *48*, 2796−2800.

(33) Taqui Khan, M. M.; Martell, A. E. *J. Am. Chem. Soc.* **1967**, *89*, 4176−4185.

(34) Kim, Y. J.; Feng, X.; Lippard, S. J. *Inorg. Chem.* **2007**, *46*, 6099−6107.

(35) (a) Singh, J.; Tabita, F. R. *J. Bacteriol.* **2010**, *192*, 1324−1331. (b) Sekowska, A.; Dénervaud, V.; Ashida, H.; Michoud, K.; Haas, D.; Yokota, A.; Danchin, A. *BMC Microbiology* **2004**, *4*, 9. (c) Imker, H. J.; Fedorov, A. A.; Fedorov, E. V.; Almo, S. C.; Gerlt, J. A. *Biochemistry* **2007**, *46*, 4077−4089.

(36) Dai, Y.; Pochapsky, T. C.; Abeles, R. H. *Biochemistry* **2001**, *40*, 6379−6387.

(37) Rubin, M. B.; Gleiter, R. *Chem. Rev.* **2000**, *100*, 1121−1164.

(38) Costas, M.; Mehn, M. P.; Jensen, M. P.; Que, L., Jr. *Chem. Rev.* **2004**, *104*, 939−986.

(39) Wray, J. W.; Abeles, R. H. *J. Biol. Chem.* **1995**, *270*, 3147−3153.

(40) Goswami, S.; Maity, A. C.; Fun, H.-K.; Chantrapromma, S. *Eur. J. Org. Chem.* **2009**, 1417−1426.

(41) No isotope incorporation from dioxygen into the ferric-oxidized products was observed in the previous study.[32]

J

dx.doi.org/10.1021/ja3038189 | *J. Am. Chem. Soc.* XXXX, XXX, XXX−XXX